Resonance-like Enhancement in high-order above-threshold ionization of polyatomic molecules

C. Wang,[1], M. Okunishi[2], X. Hao[3],* J. Chen[4,5],† Y. Yang[1], R. R. Lucchese[6], M. Zhang[1], B. Yan[1], W. D. Li[3], D. Ding[1],‡ and K. Ueda[2]§

[1]*Institute of Atomic and Molecular Physics, Jilin University, Changchun 130012, PR China*
[2]*Institute of Multidisciplinary Research for Advanced Materials, Tohoku University, Sendai 980-8577, Japan*
[3]*Institute of Theoretical Physics and Department of Physics, Shanxi University, 030006 Taiyuan, China*
[4]*CAPT, HEDPS, and IFSA Collaborative Innovation Center of MoE College of Engineering, Peking University, Beijing 100084, China*
[5]*Institute of Applied Physics and Computational Mathematics, P. O. Box 8009, Beijing 100088, China and*
[6]*Department of Chemistry, Texas A&M University, College Station, TX 77843-3255, USA*

(Dated: September 22, 2015)

We investigate the resonance-like enhancement (RLE) in high-order above-threshold ionization (ATI) spectra of the polyatomic molecules C_2H_4 and C_2H_6. In the spectrum-intensity maps, strong and weak RLE areas emerge alternatively for both C_2H_4 and C_2H_6 but in different sequences. Theoretical calculations using the strong field approximation reproduce the experimental observation and analysis shows that the different characteristics of the two molecules can be attributed to interference effects of molecular orbitals with different symmetries. For C_2H_4, the RLE structures are attributed to C-C centers of the HOMO orbital. For C_2H_6, in contrast, the C-C centers of the HOMO and HOMO-1 orbitals do not contribute to the RLE due to destructive interference but the hydrogen centers of the bonding HOMO-1 orbital give rise to the multiple RLE regions. Our work, for the first time, reveals the important role of low-lying orbitals and the differing roles of different atomic centers in the high-order ATI spectrum of molecules.

PACS numbers: 133.80.Rv, 33.80.Wz, 42.50.Hz

Imaging ultra-fast atomic and molecular dynamics and structures has been made possible by advances in the understanding of the interactions between atoms and molecules and ultrashort intense laser pulses [1, 2]. Novel methods such as laser-induced electron diffraction (LIED) [3], orbital tomography [4–7] have been developed to image molecular structures on an attosecond time scale and angstrom spatial scale. All these method are built upon the recollision mechanism [8, 9], which constitutes the foundation of our understanding of atomic and molecular dynamics in intense laser fields. For the high-energy part of the molecular above-threshold ionization (ATI) spectrum, the structure of the highest occupied molecular orbital (HOMO) has been found to play important role [10–12]. However, the low-lying molecular orbitals, whose importance have been demonstrated in molecular high harmonic generation process [6, 7], still eludes observation in the High ATI spectrum. On the other hand, though it has been widely accepted that the recollision picture can explain the overall structure of the HATI spectrum, an intriguing effect called "resonance-like enhancement (RLE)" observed in the plateau regime of the spectrum has been the source of much debate concerning its underlying mechanism but no consensus has been achieved so far [13–20]. Groups of HATI peaks (higher than $2U_p$) show unusual intensity-dependent enhancement which was at first identified for noble gas atoms: when the laser peak intensity changes only slightly, the magnitudes of HATI peaks, located at $6U_p$ and $8U_p$, can exhibit significant enhancement by up to an order of magnitude [13, 14]. Two mechanisms have been proposed to explain the RLE. In the framework of the "quantum orbits" theory, the RLE is attributed to constructive interference of a large number of electronic trajectories with small momenta when the electrons return to the ionic core which happens near channel closings [19–21]. In the Freeman resonance picture, the RLE structures originate from multiphoton resonance with intensity-dependent excited bound states [16–18]. Recently, the RLE structures were also experimentally observed for molecules [22, 23]. Analysis indicates that the mechanism favors the channel closing perspective [22].

We report on the experimental observation of the RLE structure for two hydrocarbons, C_2H_4 and C_2H_6 by measuring the HATI photoelectron spectrum. Both C_2H_4 and C_2H_6 show more than one intensity dependent RLE modulations. The magnitudes of different RLE modulations differ greatly and the weak and strong RLE modulations emerge alternately with different sequences in the two molecules. These results are reproduced by theoretical calculations and our analysis suggests that the RLE modulations of C_2H_4 come from its bonding HOMO orbital while for C_2H_6, the RLEs originate from the constructive interference of electrons emitted from the hydrogen centers of the HOMO-1 while the carbon centers in C_2H_6 do not contribute due to destructive interference.

*Electronic address: xlhao@sxu.edu.cn
†Electronic address: chen_jing@iapcm.ac.cn
‡Electronic address: dajund@jlu.edu.cn
§Electronic address: ueda@tagen.tohoku.ac.jp

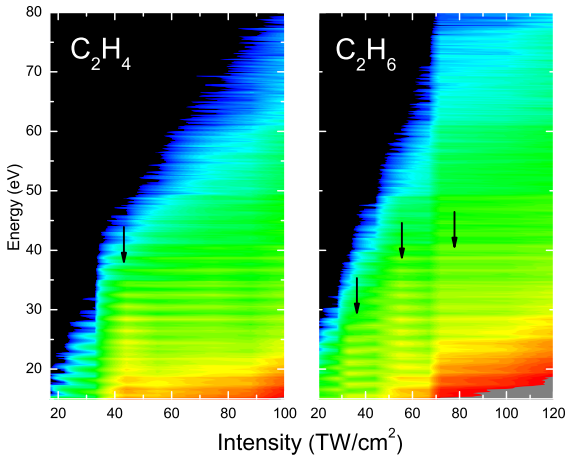

FIG. 1: (Color online) The measured ATI spectra of C_2H_4 and C_2H_6 covering a wide intensity range. The horizontal axis reflects the laser intensity and the vertical axis gives the kinetic energy of ATI electrons. The false colour scale reflects the ionization yields. The bright yellow horizontal lines indicate the RLE structures (marked by arrows)as discussed in the text.

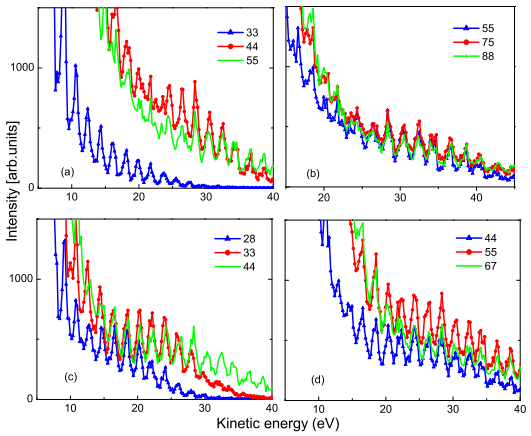

FIG. 2: (Color online) The experimental electron kinetic energy spectra of C_2H_4 (panels (a) and (b)) and C_2H_6 (panels (c) and (d)). Only the plateau regions are shown for comparison of different types of RLE. The numbers given in the legends are peak laser intensities with units of TW/cm^2.

In our experiment, we used a linear time-of-flight (TOF) (264 mm) spectrometer with a small detection solid angle ($\sim 0.0014 \times 4\pi sr$) to detect electrons. Intense 800 nm 100 fs laser pulse (repetition rate of 1 kHz) from an amplified Ti: Sapphire laser system was used to ionize molecules. The laser beam was focused by an f = 100 mm mirror to an effusively introduced C_2H_4 and C_2H_6 gas in a vacuum chamber, and a typical working pressure of 10^{-6}-10^{-8} mbar (base pressure is less than 10^{-9} mbar) ensured that space charge effects were of no consequence in our experiments. Photoelectrons were released in the filed-free interaction zone and linear polarization was along the TOF axis. The electron signal is amplified and discriminated by a CFD8 (Roentdek Handels GmbH), then the time and count information of the electron is stored by a time-to-digital converter. To estimate the peak intensity of the laser pulse, we used the well-known 10 U_p cutoff in the HATI spectra of Xe [24]. The electron energy calibration was made with reference to the multiphoton ionization of Xe atoms in the kinetic energy region of less than 10 eV, and we estimated that the error of the energy scale in our data is $< 5\%$. Further details of the experimental setup and procedure are given elsewhere [25, 26].

Figigure 1 depicts the measured ATI spectra of C_2H_4 and C_2H_6 evolving as functions of the laser intensity. To construct the 2-dimenisonal image of Fig. 1, the ATI spectrum was normalized at each laser intensity to clearly emphasize the overall evolution of the spectra with the laser intensity. The energy range ($10U_p$ cutoff) extended nearly linearly as increasing laser intensity for both molecules, indicating that the laser intensity is well below saturation. Directly ionized electrons (lower than $2U_p$) are omitted here and only high energy electrons in the plateau region are shown. Both C_2H_4 and C_2H_6 show multiple RLE features in different energy regions with increasing laser intensity. For C_2H_4, the bright yellow horizontal lines between 20-30 eV indicate that the RLE appears around 40 TW/cm^2. As can be clearly seen in Fig. 2(a), nearly a one order of magnitude enhancement is observed at 44 TW/cm^2 and then the ATI peaks are suppressed at higher intensity, e. g., 55 TW/cm^2. As the laser intensity increases, another weaker RLE modulation appears around 70 TW/cm^2 as can also be seen in Fig. 2(b). For C_2H_6, at least three RLE modulations can be seen in Fig. 1(b). Similar to C_2H_4, the weak and strong RLEs appear alternately. **The first RLE at 33 TW/cm^2 is weak whereas the second one at 55 TW/cm^2 is very strong (see Figs. 2(c) and 2(d)).**

Why do two polyatomic molecules show different types of RLE structure? As mentioned before, the mechanism responsible for the RLE is still uncertain. For atoms, both numerical solution of the time-dependent Schrödinger equation [16–18] and strong-field approximation [19–21] can reproduce the experimental observation. Thus far for molecules, only the SFA has been adopted and succeeded in explaining the appearance and absence of the RLE in N_2 and O_2 molecules [22]. To explore the underlying physics, here we employ the SFA theory to simulate the ATI spectrum. Our calculations are based on the dressed molecular strong-field approximation (SFA) in length-gauge, and details of the theory are described elsewhere [27]. In brief, the transition ampli-

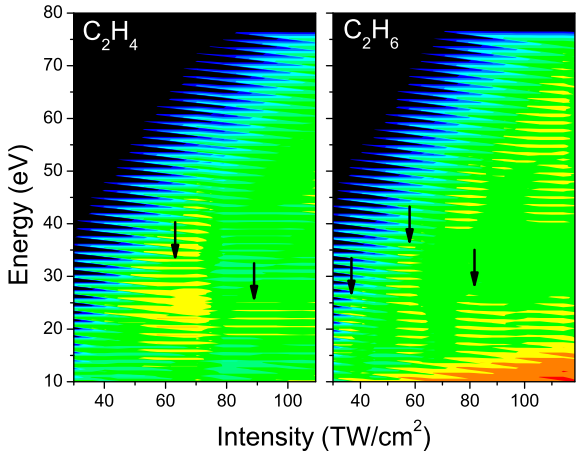

FIG. 3: (Color online) The simulated ATI spectra of C_2H_4 and C_2H_6

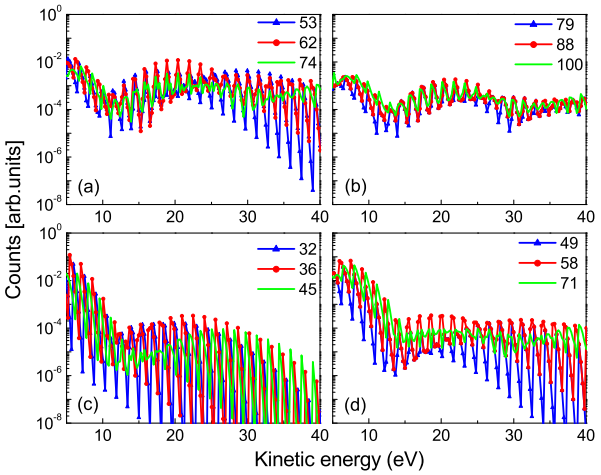

FIG. 4: (Color online) The simulated electron kinetic energy spectra of C_2H_4 (panels (a) and (b)) and C_2H_6 (panels (c) and (d)).

tude is (atomic units $m = \hbar = e = 1$ are used)

$$M_{\mathbf{p}} = M_{\mathbf{p}}^{dir} + M_{\mathbf{p}}^{resc} \tag{1}$$

where

$$M_{\mathbf{p}}^{dir} = -i \int_{-\infty}^{\infty} dt' \langle\, \psi_{\mathbf{p}}^{(V)}(t') \;\mid \mathbf{r}\cdot\; \mathbf{E}(t') \mid \psi_0(t') \,\rangle \tag{2}$$

is the amplitude for the direct electrons, and

$$M_{\mathbf{p}}^{resc} = -\int_{-\infty}^{\infty} dt \int_{-\infty}^{t} dt' \int d^3\mathbf{k} \langle\, \psi_{\mathbf{p}}^{(V)}(t) \;\; |V| \;\; \psi_{\mathbf{k}}^{(V)}(t) \,\rangle \times \langle\, \psi_{\mathbf{k}}^{(V)}(t') \;\mid \mathbf{r}\cdot\; \mathbf{E}(t') | \;\psi_0(t') \,\rangle \tag{3}$$

describes the rescattering process. Here $|\psi_0(t)\,\rangle$ is the ground state and $|\psi_{\mathbf{p}}^{(V)}(t)\,\rangle$ is the Volkov state with asymptotic momentum $\mathbf{p}$. The matrix element is calculated by the saddle-point method. For some molecules, not only the highest occupied molecular orbitals (HOMOs) but also the lower-lying orbitals can substantially contribute to the ionization process. So in our calculations, both the HOMO and HOMO-1 orbitals are included. In Table I, we show the ionization potentials of different orbitals. The difference of ionization potential between HOMO and HOMO-1 for C_2H_4 is 2 eV, indicating a dominant contribution of HOMO to the ionization of C_2H_4. Actually, according to our calculation, the transition amplitude of HOMO-1 is at least two orders of magnitude smaller than that of HOMO for C_2H_4. For C_2H_6, on the other hand, the difference is only 0.6 eV, and the contributions become comparable between HOMO-1 and HOMO. The molecular initial state $|\psi_0(t)\,\rangle$, within the fixed-nuclei approximation, can be written as a linear combination of atomic orbitals (LCAO). **Though the polyatomic molecules we consider here look very complex, they both have inversion symmetry so that the orbitals can be characterized as either g or u symmetry. The C_2H_4 molecule has D_{2h} symmetry and the C_2H_6 molecule has D_{3d} symmetry. The resulting LCAO orbitals can be written as combinations of atomic orbital pairs. In each pair, the two centers of the atomic orbitals are symmetric about the origin just as in a homonuclear diatomic molecule so that pairs of atomic orbitals form symmetric and antisymmetric combinations:**

$$\sum_a c_a \left[\; \psi_a^{(0)}(\,\mathbf{r}+\mathbf{R}_0/2) \;\pm\; \psi_a^{(0)}(\,\mathbf{r}-\mathbf{R}_0/2) \;\right], \tag{4}$$

where $\mathbf{R}_0$ denotes the relative nuclear coordinate. We show the contributions from the different centers of the molecules to the molecular orbitals in Table II. It is noted that there are two degenerate HOMOs for C_2H_6, which are distinguished by the subscript.

Table I: The ionization potentials and symmetries of the molecular orbitals.

I_p(eV)	C_2H_4	C_2H_6
HOMO	10.5 b_{3u}	11.5 e_g
HOMO-1	12.5 b_{3g}	12.1 a_{1g}

Table II: The composition of the molecular orbitals.

	C_2H_4	C_2H_6
$HOMO_1$	($Cp\pi$+$Cp\pi$)	($Cp\pi$-$Cp\pi$) +$(H+H)_1$+$(H+H)_2$-2$(H+H)_3$
$HOMO_2$		($Cp\pi$-$Cp\pi$) +$(H+H)_1$-$(H+H)_2$
HOMO-1	($Cp\sigma$-$Cp\sigma$) -$(H-H)_1$+$(H-H)_2$	($Cp\sigma$-$Cp\sigma$) -$(H+H)_1$-$(H+H)_2$-$(H+H)_3$

The simulated spectra of C_2H_4 and C_2H_6 are shown in Figs. 3 and 4. Generally, the calculation reproduces most of the features in the measurement in Figs. 1 and 2: two RLEs regions appear at around 60 TW/cm^2 and 85 TW/cm^2, respectively, in C_2H_4, whereas at least three RLEs areas appear at around 35 TW/cm^2, 60 TW/cm^2, and 85 TW/cm^2, respectively, in C_2H_6. As shown in Fig. 3, the strong and weak RLEs also emerge alternatively but with different orders for the two molecules. For C_2H_4 the first RLE is very strong and the second is weak, while for C_2H_6 the second RLE is strong and the other two are weak (see Fig. 4).

Clearly, the different RLE structures of the two molecules can be attributed to their different orbital structures. For C_2H_4, due to the dominant contribution of the HOMO of which the wave function contains only C π contributions, it is very clear that the RLE structure of C_2H_4 comes from C centers in the HOMO. For C_2H_6, the situation is much more complex. Both HOMOs and HOMO-1 contribute significantly and both C and H atomic functions are included in the wave function of all orbitals. Owing to the LCAO approximation, we can separate the contribution of different components of the wave function. In Fig. 5 we show the individual ATI spectra of HOMO and HOMO-1 of C_2H_6, and also the spectra corresponding to different components which are obtained by performing calculations with only C or H atomic orbitals included. It is noted that though here we only show the spectra for one of the degenerate HOMOs, the spectra of the other one are similar. As can be seen in Fig. 5, the RLE structure of C_2H_6 comes only from H components of HOMO-1, while C in all orbitals and H in HOMO show no RLE structure.

The appearance or absence of the RLE structure for different orbitals and cores is ascribed to the wave functions. In the view of "quantum orbits", the RLE structures originate from constructive interference of large number of multi-return orbits. **Compared to atoms, the HATI transition amplitude $M_{\mathbf{p}}^{resc}$ (Eq. (3)) of diatomic molecule contains the additional interference factor** cos $(\mathbf{k}\cdot\mathbf{R}_0/2)$ **or** sin $(\mathbf{k}\cdot\mathbf{R}_0/2)$ **corresponding to the upper and lower signs in Eq. (4), respectively[27].** Generally, electrons in multiple-return trajectories return to the core near extrema of the electric field, the intermediate momentum $\mathbf{k}$ is close to zero. **So for the orbital with a sign of "−" in Eq. (4), the above interference factor** sin $(\mathbf{k}\cdot\mathbf{R}_0/2)$ **is close to zero and there will be a suppressing effect on the RLE structure. While for the orbital with a linear combination with the "+" sign, the interference factor** cos $(\mathbf{k}\cdot\mathbf{R}_0/2)$ **is approximately equal to one and the RLE structure will survive [22].** Due to the symmetry of the polyatomic molecules considered here, they can be treated as combination of diatomic molecules as shown in Table II. Therefore the results in Figs. 3 and 5 can be understood based on the above mechanism for diatomic molecules. **For the HOMO of C_2H_4 which is dominant, the sign in Eq. (4) for the p functions on the two C centers is "+", so the RLE structure is apparently visible. But for C_2H_6, the signs of the linear combinations of the p orbitals on the C centers in both the HOMO and HOMO-1 orbitals are "−", while the corresponding signs in all H components are "+".** So the RLE structure is absent in the spectra of C cores but should be visible for H cores in all orbitals of C_2H_6. However, spectrum of the H components in HOMO$_1$, as well as in HOMO$_2$ (not shown here), of C_2H_6 shows no RLE structure. This can be attributed to the fact that these two orbitals have e_g symmetry so that, as shown in Table II, the signs in front of the pairs of H are opposite, hence their corresponding terms in the HATI transition amplitude $M_{\mathbf{p}}^{resc}$ (Eq. (3)) will cancel each other out. It is noted that this occurs exactly only when the values of interference factor corresponding to the H pairs are the same, which is only satisfied when the intermediate momentum $\mathbf{k}$=0. For non-zero $\mathbf{k}$, the factors usually are not the same since the coordinates $\mathbf{R}_0$ for the two pairs of H are different, however, they still cancel each other largely since, as mentioned before, the intermediate momentum is close to zero. The situation of HOMO$_2$ is similar but for HOMO-1, the RLE structure survives since the signs of the three pairs of H are all the same.

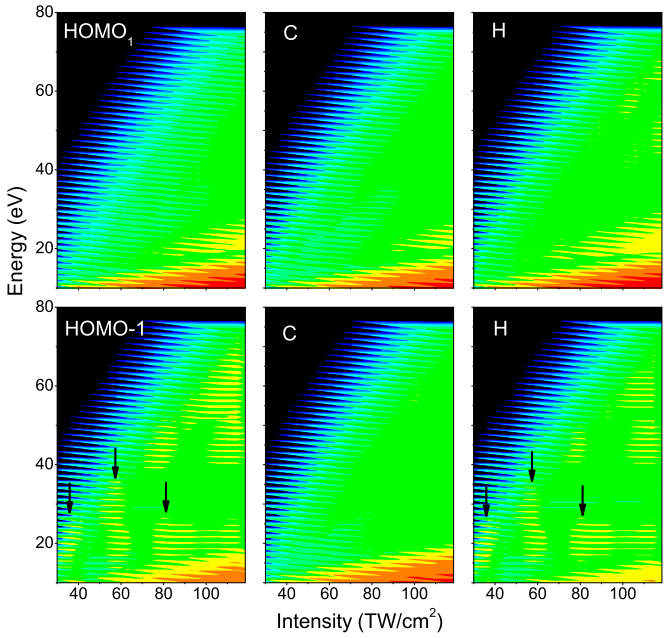

FIG. 5: (Color online) The simulated ATI spectra corresponding to different occupied orbitals of C_2H_6: HOMO$_1$ in the first row and HOMO-1 in the second row. The spectra corresponding to C and H components in each orbital are also shown in the second and third columns respectively.

According to Ref. [28], there are two different types of RLEs with different intensity dependence. The intensity dependence of the first type is comparatively smooth while that of the second type is extremely sharp. **More-**

over, the two types of RLEs appear alternatively and depend strongly on the angular momentum of the initial state. For even parity states, the sharp RLE appears at intensity corresponding to channel closing of even absorbed photon number while for odd parity states, it occurs at channel closing of odd absorbed photon number. For C_2H_4, the b_{3u} HOMO has odd parity. While for C_2H_6, both the HOMO and HOMO-1 are even parity. Though for both of C_2H_4 and C_2H_6, the photon numbers for channel closing of the first (second) RLEs are $n = 9$ ($n = 10$), they belong to different types of RLE due to different parity of the ground state. This explain why the two molecules show different sequences of strong and weak RLEs.

In conclusion, we study the resonance-like enhancement effect in strong field ionization of polyatomic molecular. We found that for C_2H_4, C-C cores in HOMO orbital are responsible for the RLE structures, while for C_2H_6, they do not contribute to RLE due to destructive interference but the hydrogen cores of the bonding HOMO-1 orbital give rise to the multiple RLEs. Our results reveals important role of low-lying orbital in the RLE and different nuclei play different role in HATI of molecules. Moreover, our work provides clear experimental evidence of the existence of two types of the RLE and their dependence on the parity of ground state. This work sheds important new light into laser assisted ultrafast imaging of molecules.

This work was partially supported by the National Basic Research Program of China Grant (No. 2013CB922200 and No. 2011CB808102), NNSFC (No. 11304117, No.11304329, No. 11175227, No. 11105205, 11274050, 11334009 and 11425414), the China Postdoctoral Science Foundation under Grant No.2013M530137, and by IMRAM project.

[1] C. I. Blaga, J. Xu, A. D. DiChiara, E. Sistrunk, K. Zhang, P. Agostini, T. A. Miller, L. F. DiMauro, and C. D. Lin, Nature (London) 483, 194 (2012).
[2] P. Salières, A. Maquet, S. Haessler, J. Caillat, and R. TAïeb, Rep. Prog. Phys. 75, 062401 (2012).
[3] M. Meckel, D. Comtois, D. Zeidler, A. Staudte, D. Pavičić, H. C. Bandulet, H. Pépin, J. C. Kieffer, R. Dörner, D. M. Villeneuve and P. B. Corkum, Science 320, 1478 (2008)
[4] J. Itatani, J. Levesque, D. Zeidler, H. Niikura, H. Pepin, J. C. Kieffer, P. B. Corkum, and D. M. Villeneuve, Nature (London) 432, 867 (2004).
[5] C. Vozzi, M. Negro, F. Calegari, G. Sansone, M. Nisoli, S. De Silvestri, and S. Stagira, Nat. Phys. 7, 822 (2011).
[6] B. K. McFarland, J. P. Farrell, P. H. Bucksbaum, and M. Ghr, Science 322, 1232 (2008).
[7] O. Smirnova, Y. Mairesse, S. Patchkovskii, N. Dudovich, D. Villeneuve, P. Corkum, and M. Y. Ivanov, Nature (London) 460, 972 (2009).
[8] P. B. Corkum, Phys. Rev. Lett. 71, 1994 (1993).
[9] K. J. Schafer, B. Yang, L. F. DiMauro, and K. C. Kulander, Phys. Rev. Lett. 70, 1599 (1993)
[10] M. Okunishi, R. Itaya, K. Shimada, G. Prümper, K. Ueda, M. Busuladžić, A. Gazibegovicć-Busuladžić, D. B. Milošević, and W. Becker, Phys. Rev. Lett. 103, 043001 (2009).
[11] H. Kang *et al.*, Phys. Rev. Lett. **104**, 203001 (2010).
[12] M. Okunishi, H. Niikura, R. R. Lucchese, T. Morishita and K. Ueda, Phys. Rev. Lett. 106, 063001 (2011).
[13] M. P. Hertlein, P. H. Bucksbaum, and H. G. Muller, J. Phys. B **30**, L197 (1997).
[14] P. Hansch, M. A. Walker and L. D. Van Woerkom, Phys. Rev. A 55, R2535 (1997).
[15] F. Grasbon, G. G. Paulus, H. Walther, P. Villoresi, G. Sansone, S. Stagira, M. Nisoli, and S. De Silvestri, Phys. Rev. Lett. 91,173003 (2003).
[16] H. G. Muller and F. C. Kooiman, Phys. Rev. Lett. 81, 1207 (1998).
[17] H. G. Muller, Phys. Rev. Lett. 83, 3158 (1999).
[18] J. Wassaf, V. Véniard, R. Taïeb, and A.Maquet, Phys. Rev. Lett. 90, 013003 (2003).
[19] R. Kopold and W. Becker, J. Phys. B **32**, L419 (1999).
[20] S. V. Popruzhenko, Ph. A. Korneev, S. P. Goreslavski, and W. Becker, Phys. Rev. Lett. **89**, 023001 (2002).
[21] G. G. Paulus, F. Grasbon, H. Walther, R. Kopold, and W. Becker, Phys. Rev. A **64**, 021401(R) (2001).
[22] W. Quan, X. Lai, Y. Chen, C. Wang, Z. Hu, X. Liu, X. Hao, J. Chen, E. Hasović, M. Busuladžić, W. Becker and D. B. Milošvić, Phys. Rev. A. 88, 021401(R) (2013).
[23] C. Wang, Y. Tian, S. Luo, W.G. Roeterdink, Y. Yang, D. Ding, M. Okunishi, G. Prumper, K. Shiamada,R. Zhu and K. Ueda, Phys. Rev. A. 90, 023405 (2013).
[24] G.G. Paulus, W. Becker, W. Nicklich and H. Walther, J. Phys. B **27**, L703 (1994).
[25] M. Okunishi, K. Shiamada, G. Prümper, D. Mathur, and K. Ueda, J. Chem. Phys. 127, 064310 (2007).
[26] C. Wang, M. Okunishi, R. R. Lucchese, T. Morishita, O. I. Tolstikhin, L. B. Madsen, K. Shimada, D. Ding and K. Ueda, J. Phys. B: At. Mol. Opt. Phys. 45, 131001 (2012).
[27] D. B. Milošević,Phys. Rev. A **74**, 063404 (2006); M. Busuladžić, A. Gazibegović-Busuladžić, D. B. Milošević and W. Becker, Phys. Rev. Lett. **100**, 203003 (2008); Phys. Rev. A **78**, 033412 (2008).
[28] D. B. Milošević, E. Hasović, M. Busuladžić, A. Gazibegović-Busuladžić and W. Becker, Phys. Rev. A **76**, 053410 (2007).